

Variation of ferroelectric properties in (Bi,Pr)(Fe,Mn)O₃/SrRuO₃-Pt/CoFe₂O₄ layered film structure by applying direct current magnetic field

メタデータ	言語: eng 出版者: 公開日: 2022-01-24 キーワード (Ja): キーワード (En): 作成者: メールアドレス: 所属:
URL	https://doi.org/10.24517/00064705

This work is licensed under a Creative Commons Attribution-NonCommercial-ShareAlike 3.0 International License.



Variation of ferroelectric properties in (Bi,Pr) (Fe,Mn)O₃/SrRuO₃-Pt/CoFe₂O₄ layered film structure by applying direct current magnetic field

Cite as: J. Appl. Phys. **111**, 124103 (2012); <https://doi.org/10.1063/1.4730334>

Submitted: 29 March 2012 • Accepted: 19 May 2012 • Published Online: 20 June 2012

Chen Liu, Takeshi Kawai, Yoshinori Tsukada, et al.



View Online



Export Citation

ARTICLES YOU MAY BE INTERESTED IN

[Multiferroic magnetoelectric composites: Historical perspective, status, and future directions](#)
Journal of Applied Physics **103**, 031101 (2008); <https://doi.org/10.1063/1.2836410>

[Optimizing direct magnetoelectric coupling in Pb\(Zr,Ti\)O₃/Ni multiferroic film heterostructures](#)

Applied Physics Letters **106**, 072901 (2015); <https://doi.org/10.1063/1.4913471>

[Ultra-sensitive NEMS magnetoelectric sensor for picotesla DC magnetic field detection](#)
Applied Physics Letters **110**, 143510 (2017); <https://doi.org/10.1063/1.4979694>



Applied Physics
Reviews

Read. Cite. Publish. Repeat.

19.162

2020 IMPACT FACTOR*

Variation of ferroelectric properties in (Bi,Pr)(Fe,Mn)O₃/SrRuO₃-Pt/CoFe₂O₄ layered film structure by applying direct current magnetic field

Chen Liu,¹ Takeshi Kawae,^{1,a)} Yoshinori Tsukada,¹ Akiharu Morimoto,¹ Hiroshi Naganuma,² Takashi Nakajima,³ and Soichiro Okamura³

¹Graduate School of Natural Science and Technology, Kanazawa University, Kakuma-machi, Kanazawa, Ishikawa 920-1192, Japan

²Department of Applied Physics, Graduate School of Engineering, Tohoku University, Aoba 6-6-05, Aramaki, Aoba-ku, Sendai 980-8579, Japan

³Department of Applied Physics, Faculty of Science, Tokyo University of Science, Shinjuku-ku, Tokyo 162-8601, Japan

(Received 29 March 2012; accepted 19 May 2012; published online 20 June 2012)

We report the preparation of (Bi,Pr)(Fe,Mn)O₃(BPFM)/SrRuO₃ (SRO)-Pt/CoFe₂O₄(CFO) layered film structure on (100) SrTiO₃ substrate by pulsed laser deposition method and their structural and electrical properties. Favorable ferroelectric properties of BPFM were observed in the layered film structure with (100)-oriented growth of BPFM, SRO, and CFO. Variation of polarization vs electric field loops of BPFM by applying DC magnet field was observed, and the remnant polarization was found to increase by 3% with increasing the applied magnetic field from 0 to 10 kOe. The magnetoelectric coefficient in the present structure was estimated to be 1.5 V/(cmOe). © 2012 American Institute of Physics. [<http://dx.doi.org/10.1063/1.4730334>]

I. INTRODUCTION

Multiferroic materials, which exhibit simultaneous ferroelectric and ferromagnetic behaviors, have attracted much attention for innovative electronic device application in data storage, sensors, and actuators.¹⁻⁵ Multiferroic materials are capable of producing magnetoelectric (ME) effect which exhibit an induced polarization (magnetization) under external magnetic field (electric field).¹⁻⁹ However, it is not easy to realize the coexistence of sufficient ferroelectric and ferromagnetic properties in the single-phase materials,^{2,7} although the ME effect has a long research history since the discovery in Cr₂O₃ in 1960s.^{4,5} Compared with single-phase material, mixing ferroelectric material with ferromagnetic one into composite is an effective and simple route to achieve multiferroic properties at room temperature.⁹⁻¹⁴ In addition, the composite multiferroic materials are capable of producing the ME effect through the strain-coupling between the ferroelectric and ferromagnetic phases.⁹⁻¹⁴

In recent years, the most widely studied composite multiferroic materials are nanopillars and layered film structure.¹⁴ The self-assembled composite films consist of ferromagnetic nanopillars embedded in a ferroelectric matrix. In self-assembled composite films, it is not easy to observe sufficient ME effect due to leakage current through the low-resistive ferromagnetic parts and impurity phases.¹⁴⁻¹⁷ On the other hand, the ME effect in layered film structure is expected to be superior to nanopillars structure since the ferroelectric layer can easily be electrically poled without influences of low-resistive ferromagnetic parts and impurity phase in the composite structure.¹⁸⁻²¹

In past, we have proposed a simple artificially layered film structure consisting of ferroelectric BiFeO₃ (BFO),

bottom electrode Pt, and ferromagnetic CoFe₂O₄ (CFO), and prepared that structure on a SrTiO₃ (STO) substrate by pulsed laser deposition.²² Due to the electrical separation of the BFO and CFO in the structure, an efficient application of the electric field to the BFO was realized. As a result, the well-saturated hysteresis loops in the polarization vs electric field (*P-E*) and magnetization vs magnetic field (*M-H*) curves coexisted at room temperature. CFO is known to have a large magnetostriction constant in oxide ferromagnetic materials. Therefore, in that structure, it is expected that CFO provides a large stress to BFO by applying the magnetic field, suggesting a large ME effect through the strain-coupling. In the composite multiferroic materials, there have been several reports concerning the modulation of electric polarization and dielectric constant in the material by AC magnetic field.^{3,4,9,14} However, changes of electric polarization by applying the DC magnetic field have not been reported in the literature. Therefore, in this work, we report a variation of the electrical polarization in artificially layered film structure by applying the DC magnetic field.

II. EXPERIMENTAL DETAILS

For large strain-coupling between BFO and CFO, small lattice mismatch between the materials in the layered film structure is required. We have chosen pseudo-perovskite SrRuO₃ (SRO) as a bottom electrode material, because of the small lattice mismatch between BFO and SRO (lattice mismatch 0.75%). For suppression of the leakage current in the BFO thin film, we have used (Pr, Mn)-codoped BFO (BPFM) as a ferroelectric material.²³ BPFM, SRO, and CFO films were deposited on the (100) STO substrates by pulsed laser deposition (PLD). On the other hand, it is difficult to crystallize the SRO on the CFO due to a large lattice mismatch between SRO and CFO (lattice mismatch 5.3%). Since the epitaxial growth of Pt on the CFO has reported in

^{a)}Author to whom correspondence should be addressed. Electronic mail: kawae@ec.t.kanazawa-u.ac.jp.

our previous work,²² ultrathin Pt (less than 5 nm) seed layer was deposited on the CFO for crystallizing the SRO. Sintered ceramics with compositions of $(\text{Bi}_{1.0}\text{Pr}_{0.1})(\text{Fe}_{0.97}\text{Mn}_{0.03})\text{O}_3$, SrRuO_3 , and CoFe_2O_4 were used as PLD targets for BPFM, SRO, and CFO films, respectively. The detailed deposition conditions and film thickness of BPFM, SRO, Pt, and CFO are summarized in Table I. For comparison, we have prepared the BPFM film on the SRO-coated STO substrate without CFO film and investigated their properties. Au top electrodes were deposited by thermal evaporation on the surface of BPFM film, resulting in the metal-insulator-metal capacitors structure.

The crystal structure of specimen was determined by x-ray diffraction (XRD) with Cu $K\alpha$ radiation θ - 2θ using XD-D1 (Shimadzu). The ferroelectric properties were measured by using ferroelectric test system FCE-3 (Toyo). For characterization of ME effect in the present structure, the ferroelectric properties were measured with applying the DC magnetic field (0 to 10 kOe) at room temperature. Then, the magnetic field was applied to the specimen along the in-plane direction by using the vibrating sample magnetometer VSM-5 (Tamakawa).

III. RESULTS AND DISCUSSION

Figure 1 shows the XRD patterns of the BPFM/SRO-Pt/CFO layered film and the BPFM/SRO film on the STO substrate. As shown in Fig. 1(a), in the BPFM/SRO-Pt/CFO layered film, the BPFM, SRO, and CFO were (100)-oriented on the STO substrate without impurity phases and other orientations. It seems that the BPFM and SRO were epitaxially grown on the CFO due to the ultrathin Pt seed layer in the present structure. Also, in the BPFM/SRO layered film, both BPFM and SRO show (100)-orientation on the STO substrate.

Figure 2(a) shows the P - E curves of film capacitors measured with 5 kHz at room temperature. The BPFM/SRO-Pt/CFO layered film indicates well saturated hysteresis loop, which is almost same as that of the BPFM/SRO layered film. Furthermore, as shown in Fig. 2(b), the leakage current of the BPFM/SRO-Pt/CFO layered film is almost same as that of the BPFM/SRO layered film. These results indicate that the ferroelectric properties in the BPFM film are maintained even in the CFO-coated STO substrate. The remnant polarization $2P_r$ and the coercive field $2E_c$ in the BPFM/SRO-Pt/CFO layered film were approximately $100 \mu\text{C}/\text{cm}^2$ and $520 \text{ kV}/\text{cm}$ at the maximum electric field of $750 \text{ kV}/\text{cm}$, respectively.

TABLE I. Deposition conditions and thickness for BPFM, SRO, Pt, and CFO films.

	BPFM	SRO	Pt	CFO
Laser	KrF excimer (248 nm)			
Laser energy (mJ)	100	120	130	130
Repetition rate (Hz)	5	2	5	5
Substrate temperature ($^{\circ}\text{C}$)	600	700	600	700
O_2 pressure during deposition (Torr)	0.1	0.1	Vac.	0.03
Thickness (nm)	360	30	<5	200

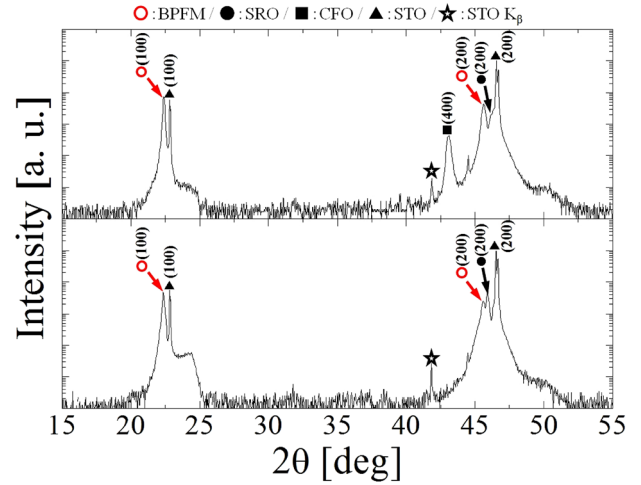


FIG. 1. XRD patterns for (a) BPFM/SRO-Pt/CFO layered film and (b) BPFM/SRO layered film on the STO substrates.

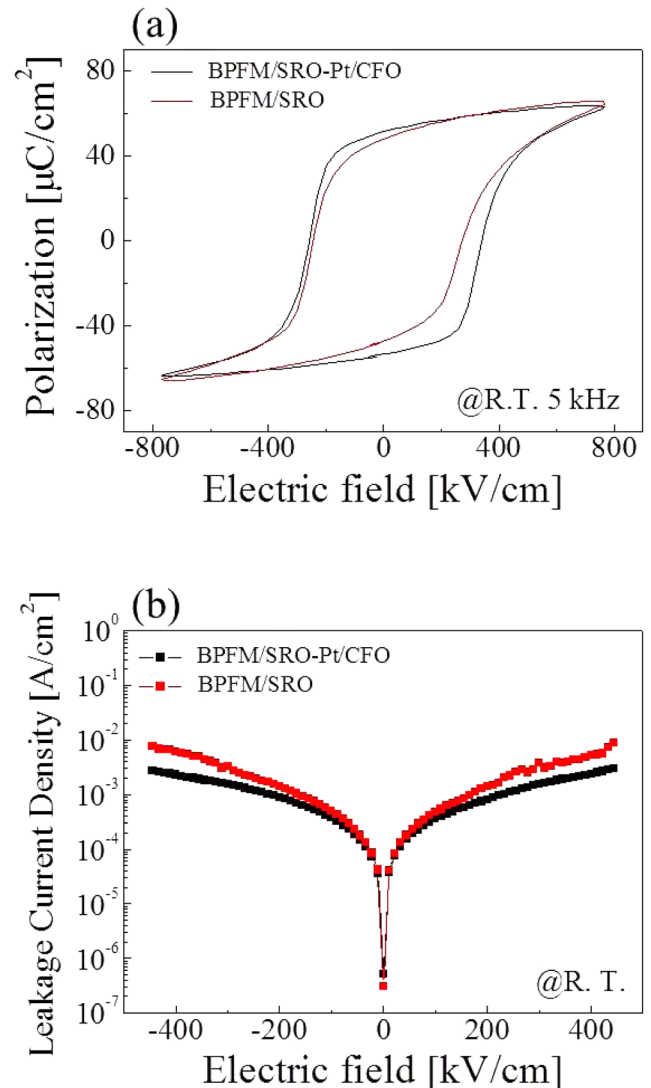


FIG. 2. (a) P - E and (b) J - E curves for BPFM/SRO-Pt/CFO layered film and BPFM/SRO layered film on the STO substrates.

In ferroelectrics, it is occasionally observed that the remnant polarization and coercive field are changed with initial multiple applications of the electric field, and then those are stabilized. This phenomenon might be caused by instability of domain wall pinning sites.²⁴ As mentioned later, in the measurement of the ME effect for specimen, P - E curves were repeatedly measured under the magnetic field. Hence, it is difficult to judge the origin (ME effect or not) for slight change of remnant polarization and coercive field under the magnetic fields. Thus, we investigated the number of applied electric field cycles dependence of $2P_r$ and $2E_c$ in the specimen. As shown in Fig. 3, $2P_r$ and $2E_c$ rapidly decrease during the region of 0 to 20 cycles, and then $2P_r$ and $2E_c$ are almost kept constant with variation of 0.1%–0.3%. Hence, for investigation of the ME effect, the magnetic field dependences of P - E curves were measured after applying the bipolar electric field of 500 kV/cm with 20 cycles.

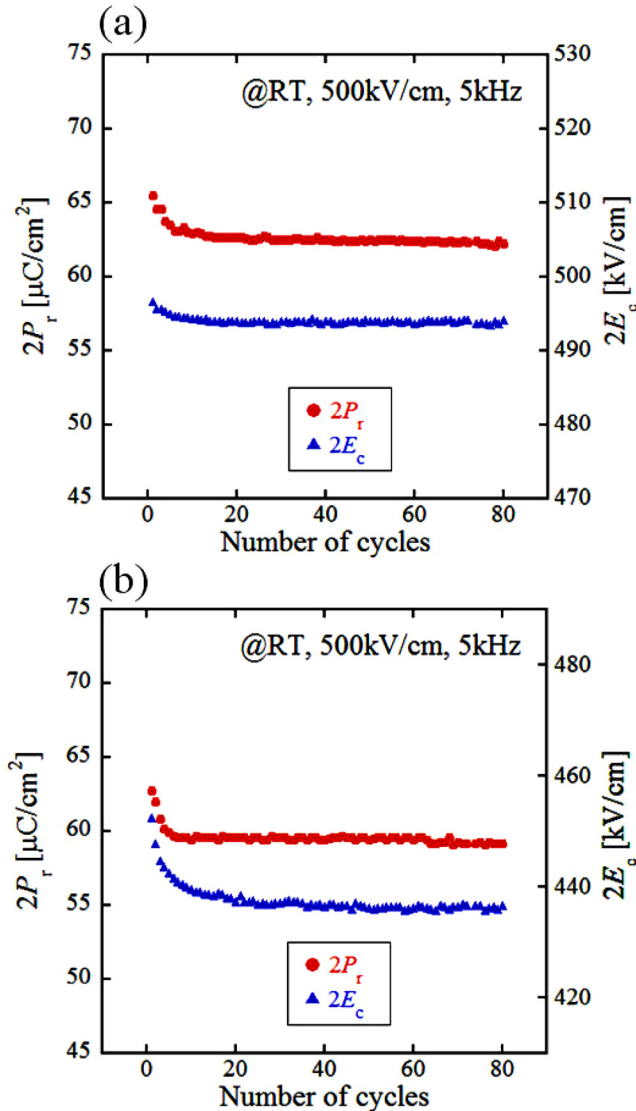


FIG. 3. $2P_r$ and $2E_c$ as a function of number of applied electric field cycles for (a) BPFM/SRO-Pt/CFO layered film and (b) BPFM/SRO layered film on the STO substrates.

Figure 4 shows the P - E curves of specimen at the maximum electric field of 500 kV/cm with and without magnetic field of 10 kOe. As shown in Figs. 4(a) and 4(b), in the BPFM/SRO-Pt/CFO layered film, the polarization value in the curve was increased by applying the magnetic field. Increments of $2P_r$, polarization at maximum electric field $2P_m$, and maximum polarization in the curve $2P_M$ were 2.0, 1.8, and 1.8 $\mu\text{C}/\text{cm}^2$, respectively. By contrast, as shown in Figs. 4(c) and 4(d), in the BPFM/SRO layered film on the STO substrate, no changes of P - E curves by applying the magnetic field were observed.

Figures 5(a) and 5(b) show the applied magnetic field dependence of $2P_r$ and $2E_c$ of BPFM/SRO-Pt/CFO layered film. With increasing the applied magnetic field, $2P_r$ was linearly increased while $2E_c$ was not changed. Then, the observed variation of $2E_c$ under the magnetic field is only 0.2%, which is equivalent to the error limits above 20 cycles shown in the Fig. 3(a). On the other hand, $2P_r$ was found to be increased by 3% at the maximum magnetic field of 10 kOe, which is 10 times larger than the error limits. In addition, $2P_r$ was reversibly decreased when the applied magnetic field was decreased from 10 to 0 kOe as shown in the figure. In the case of BPFM/SRO layered film on the STO substrate, neither $2P_r$ nor $2E_c$ was not changed with applying the magnetic field (shown in Figs. 5(c) and 5(d)), and the variations of $2P_r$ and $2E_c$ under magnetic field were only 0.3%–0.5%, suggesting that the ME effect in BPFM/SRO layered film is unable to be observed with magnetic fields less than 10 kOe.

As origin of observed increase of polarization by applying the magnetic field, we consider it is mainly caused by the strain transfer from CFO to BPFM in the present structure. At first, by applying the magnetic field along the in-plane direction, CFO shows in-plane compressive strain due to the negative magnetostriction constant of CFO.²⁵ Then, the compressive strain of CFO provides in-plane compressive stress to the BPFM film through the SRO-Pt layer. Subsequently, BPFM film has in-plane compressive and out-of-plane tensile stress, indicating the tetragonal distortion. The unit cell of the BPFM is expanded to the out-of-plane direction. As a result, the polarization induced by electric field along the out-of-plane direction was enhanced by expanding of the unit cell due to the strain transfer.^{26,27} Accordingly, we conclude that the present BPFM/SRO-Pt/CFO layered film showed the ME effect through the strain-coupling.

ME coefficient α_E of multiferroelectric materials was generally defined as an equation $\alpha_E = \Delta E / \Delta H$, where ΔH and ΔE are the change in the applying AC magnetic field and the corresponding change under the AC magnetic field, respectively.¹⁴ Here, to determine the DC α_E of the present structure, ΔE was estimated by applied electric field (E) dependence of $2P_r$ without magnetic field shown in the inset to Fig. 6. Using the linear fit of E - $2P_r$ curve ($2P_r = 0.1124E + 1.284$), ΔE was estimated via the change in $2P_r$ ($\Delta 2P_r$) for deviation of applied magnetic field (ΔH). Estimated α_E of BPFM/SRO-Pt/CFO layered thin films as a function of the applied magnetic field is shown in Fig. 6. As can be seen, regardless of the applied magnetic field, the ME

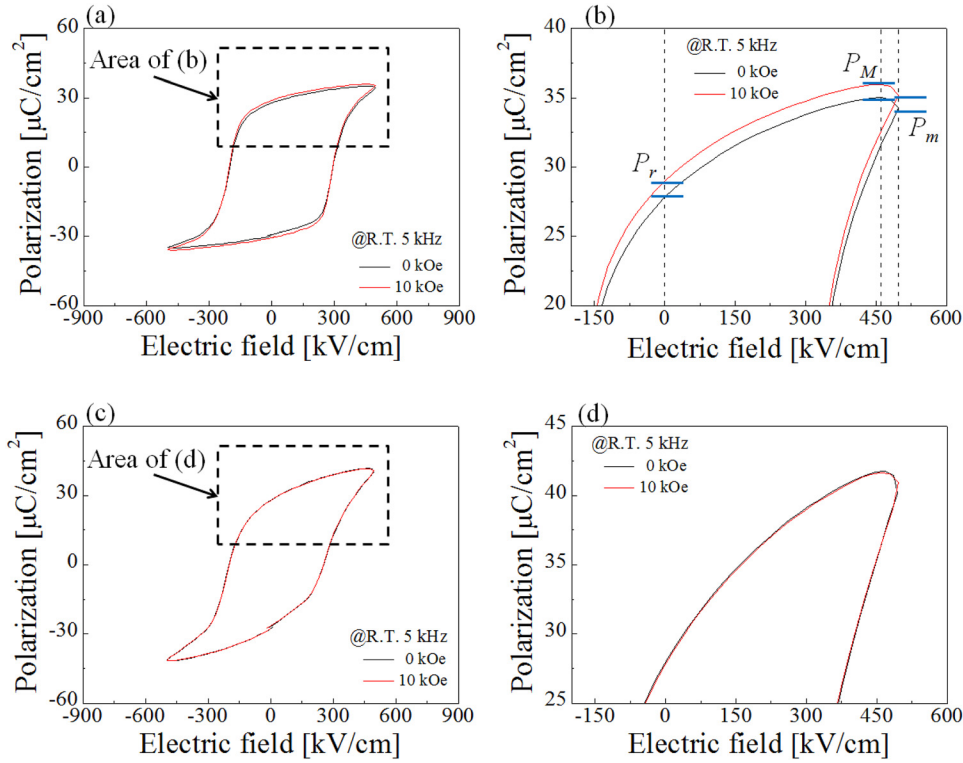


FIG. 4. P - E curves at the maximum electric field of 500kV/cm with and without magnetic field of 10 kOe for (a) and (b) BPFM/SRO-Pt/CFO layered film and (c) and (d) BPFM/SRO layered film on the STO substrates.

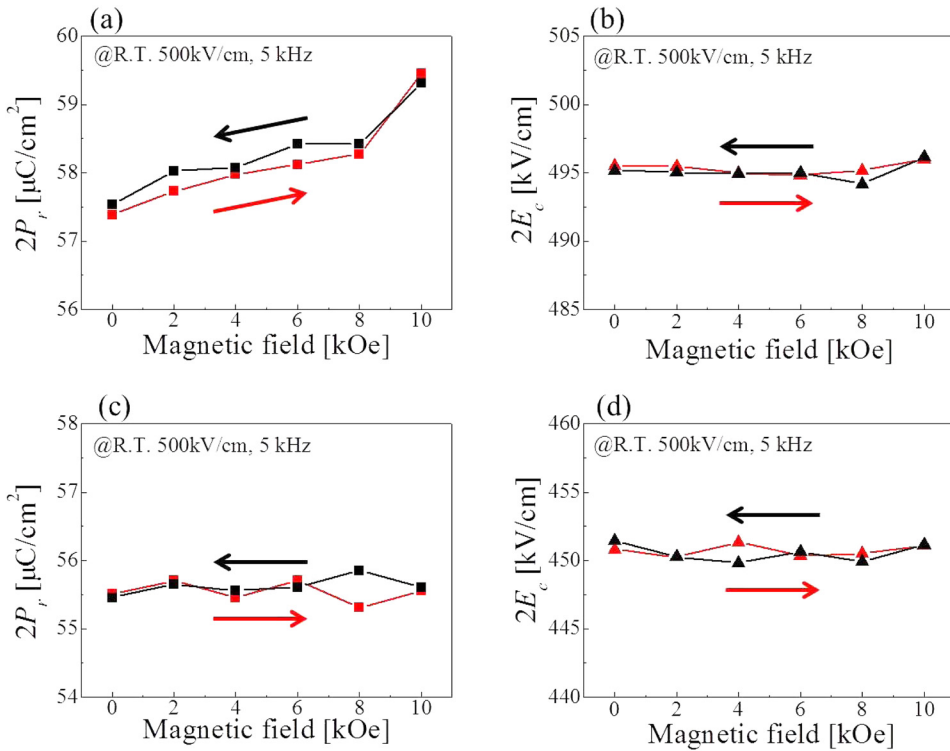


FIG. 5. Applied magnetic field dependence of $2P_r$ and $2E_c$ for (a) and (b) BPFM/SRO-Pt/CFO layered film and (c) and (d) BPFM/SRO layered film on the STO substrates.

coefficient was about 1.5 V/(cmOe). That agrees with simple increase of $2P_r$ for the applied magnetic field shown in Fig. 5(a).

In order to realize the large ME coefficient in the present structure, it is required to enhance the strain-coupling between BFO and CFO. For that requirement, bottom electrode film (serving as a buffer layer) must satisfy both thinner structure and good conductivity. In addition, it is

necessary to investigate the microstructure (especially, interface state) of layered films by using direct observation techniques such as HR-TEM since the defects in the interface easily degrade the mechanical coupling of each layer. Hence, it is required to investigate the influences of bottom electrode thickness on both strain-coupling and ferroelectricity, through the characterization of microstructure of specimen.

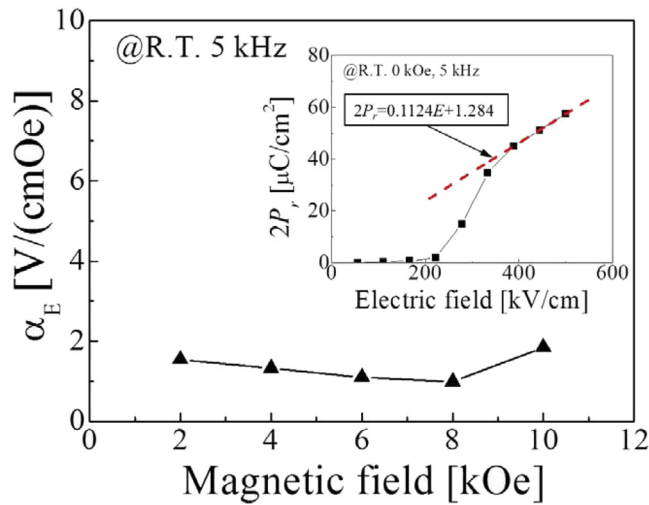


FIG. 6. Magnetic field dependence of ME coefficient at room temperature. The inset shows electric field dependence of $2P_r$, without magnetic field.

IV. CONCLUSION

We have prepared the BPFM/SRO-Pt/CFO layered thin films on the STO substrate by PLD method and investigated its structural and electrical properties. BPFM, SRO, and CFO showed (100)-oriented growth on the STO substrate without impurity phases and other orientation components, and favorable ferroelectric properties of BPFM in the layered film structure were observed. By applying the DC magnet field, the variation of P - E curves was observed, and the $2P_r$ increases by 3% at the maximum applied magnetic field of 10 kOe. Accordingly, in BPFM/SRO-Pt/CFO layered thin films, the strain-coupling ME effect was observed, and the ME coefficient was estimated to be 1.5 V/(cmOe).

ACKNOWLEDGMENTS

The authors would like to thank Mr. Y. Nomura, Dr. T. Ueno, and Professor S. Yamada of Kanazawa University for their fruitful discussions and technical supports.

- ¹W. Eerenstein, N. D. Mathur, and J. F. Scott, *Nature* **442**, 17 (2006).
- ²B. B. V. Aken, J.-P. Rivera, H. Schmid, and M. Fiebig, *Nature* **449**, 702 (2007).
- ³Z. Cheng and X. Wang, *Phys. Rev. B* **75**, 172406 (2007).
- ⁴L. Yan, Z. Xing, Z. Wang, T. Wang, G. Lei, J. Li, and D. Viehland, *J. Appl. Phys.* **107**, 064106 (2010).
- ⁵D. N. Astrov, *Zh. Eksp. Teor. Fiz.* **11**, 708 (1960).
- ⁶G. T. Rado and V. J. Folen, *Phys. Rev. Lett.* **7**, 310 (1961).
- ⁷J. Wang, J. B. Neaton, H. Zheng, V. Nagarajan, S. B. Ogale, B. Liu, D. Viehland, V. Vaithyanathan, D. G. Schlom, U. V. Waghmare, N. A. Spaldin, K. M. Rabe, M. Wuttig, and R. Ramesh, *Science* **299**, 1719 (2003).
- ⁸S. Goswami, D. Bhattacharya, P. Choudhury, B. Ouladdiaf, and T. Chatterji, *Appl. Phys. Lett.* **99**, 073106 (2011).
- ⁹J. Wu and J. Wang, *J. Appl. Phys.* **105**, 124107 (2009).
- ¹⁰J. Wang, H. Zhang, X. Wang, D. Pan, J. Liu, and G. Wang, *Appl. Phys. Lett.* **89**, 122914 (2006).
- ¹¹J. Ryu, A. V. Carazo, K. Uchino, and H. E. Kim, *Jpn. J. Appl. Phys., Part 1* **40**, 4948 (2001).
- ¹²C. W. Nan, *Phys. Rev. B* **50**, 6082 (1994).
- ¹³S. X. Dong, J. F. Li, and D. Viehland, *Appl. Phys. Lett.* **83**, 2265 (2003).
- ¹⁴H. Zheng, J. Wang, S. E. Lofland, Z. Ma, L. Mohaddes-Arbabili, T. Zhao, L. Salamanca-Riba, S. R. Shinde, S. B. Ogale, F. Bai, D. Viehland, Y. Jia, D. G. Schlom, M. Wuttig, A. Roytburd, and R. Ramesh, *Science* **303**, 30 (2004).
- ¹⁵H. Zheng, F. Straub, Q. Zhan, P. L. Yang, W. K. Hsieh, F. Zavaliche, Y. H. Chu, U. Dahmen, and R. Ramesh, *Adv. Mater.* **18**, 2747 (2006).
- ¹⁶H. Zheng, Q. Zhan, F. Zavaliche, M. Sherburne, F. Straub, M. O. Cruz, L. Q. Chen, U. Dahmen, and R. Ramesh, *Nano Lett.* **6**, 1401 (2006).
- ¹⁷C. W. Nan, G. Liu, and Y. Lin, *Phys. Rev. Lett.* **94**, 197203 (2005).
- ¹⁸G. Srinivasan, E. T. Rasmussen, J. Gallegos, and R. Srinivasan, *Phys. Rev. B* **64**, 214408 (2001).
- ¹⁹M. Murakami, K. S. Chang, M. A. Aronova, C. L. Lin, M. H. Yu, J. Hattrick-Simpers, M. Wuttig, I. Takeuchi, C. Gao, B. Hu, S. E. Lofland, L. A. Knauss, and L. A. Bendersky, *Appl. Phys. Lett.* **87**, 112901 (2005).
- ²⁰M. Ziese, A. Bollero, I. Panagiotopoulos, and N. Moutis, *Appl. Phys. Lett.* **88**, 212502 (2006).
- ²¹H. C. He, J. P. Zhou, J. Wang, and C. W. Nan, *Appl. Phys. Lett.* **89**, 052904 (2006).
- ²²T. Kawae, J. Hu, H. Naganuma, T. Nakajima, Y. Terauchi, S. Okamura, and A. Morimoto, *Thin Solid Films* **519**, 7727 (2011).
- ²³T. Kawae, Y. Terauchi, T. Nakajima, S. Okamura, and A. Morimoto, *J. Ceram. Soc. Jpn.* **118**, 652 (2010).
- ²⁴A. Z. Simoes, L. S. Cavalcante, F. Moura, E. Longo, and J. A. Varela, *J. Alloys Compd.* **509**, 5326 (2011).
- ²⁵R. M. Bozorth, E. F. Tilden, and A. J. Williams, *Phys. Rev.* **99**, 1788 (1955).
- ²⁶J. X. Zhang, J. Y. Dai, C. K. Chow, C. L. Sun, V. C. Lo, and H. L. W. Chan, *Appl. Phys. Lett.* **92**, 022901 (2008).
- ²⁷M. D. Biegalski, D. H. Kim, S. Choudhury, L. Q. Chen, H. M. Christen, and K. Dorr, *Appl. Phys. Lett.* **98**, 142902 (2011).